Supplementary Information for

Cortical route for facelike pattern processing in human newborns

Marco Buiatti, Elisa Di Giorgio, Manuela Piazza, Carlo Polloni, Giuseppe Menna, Fabrizio Taddei, Ermanno Baldo, Giorgio Vallortigara

Correspondence should be addressed to:
Marco Buiatti (marco.buiatti@unitn.it) or
Giorgio Vallortigara (giorgio.vallortigara@unitn.it).

This PDF file includes:

SI Materials and Methods
Figs. S1, S2, S3

www.pnas.org/cgi/doi/10.1073/pnas.1812419116

SI Materials and Methods

Stimuli. Stimuli were presented using the Psychtoolbox 3.0.12 (1, 2) for Windows in Matlab R2014a (Natick, MA). Visual stimuli (Fig. 1, top panel) consisted of a white head-shaped form, 14.2 cm × 22 cm (25° × 38°) containing three black squares (2.5 cm × 2.5 cm, 4.4° × 4.4°), and differed only for the spatial configuration of the three squares. In the face stimulus, the squares were placed in the appropriate location for the eyes and the mouth to form an upright facelike pattern resembling a schematic human face; in the inverted face stimulus, the spatial configuration of the squares was rotated by 180°; the scrambled face stimulus was obtained from the face stimulus by shifting the two upper squares on one side and the lower square on the opposite side of the head shape (sides were counterbalanced across subjects).

Stimuli were presented dynamically with sinusoidal contrast modulation (0-100%) at a rate of 0.8 Hz (1 cycle = 1.25 s) overlapped onto a weakly contrasted dynamic background (Fig. 1, bottom panel) consisting of a flickering white noise image (a rectangle, 45 cm x 33.8 cm, where the color of each pixel varies randomly between mid-gray (b/w intensity = 128/256) and grayish white (b/w intensity = 223/256) at a frequency of 3.75 Hz).

EEG recordings. EEG was recorded with an EGI EEG system (GES400, Electrical Geodesic, Inc, Eugene, OR, USA) including a high-density (125 electrodes) cap (Geodesic Sensor Net) specifically built for newborns (compatible with head circumference between 34 and 36 cm) and allowing easy, fast and comfortable application (contact with the scalp is made with wet sponges soaked in saline solution). Scalp voltages were referenced to the vertex, amplified and digitized at 250 Hz.

EEG data preprocessing. EEG preprocessing was performed with EEGLAB (3). EEG data were band-pass filtered between 0.1 and 40 Hz and segmented in blocks corresponding to fixation intervals. Bad channels were identified with the help of the TrimOutlier (https://sccn.ucsd.edu/wiki/TrimOutlier) toolbox by excluding channels that had a standard deviation higher than 150 μV or lower than 1 μV or that showed artefactual patterns at visual inspection (on average 4.9 per subject, min 0, max 14). Signals of bad channels were replaced with interpolated signals from neighbouring channels (standard spherical interpolation method in EEGLAB). Data segments containing amplitudes exceeding ±200 μV or containing paroxysmic artifacts after visual inspection were rejected. Continuous data blocks shorter than 10 s (the minimum duration required for the frequency-tagging analysis, see below) were excluded. The resulting signals were mathematically referenced to the average of the 125 channels.

Source reconstruction. As a head model, we used the one described in (4) (details therein). In brief, a realistic head model was generated from the anatomical magnetic resonance images (MRI) of a healthy full-term baby. The three-shell physical model included scalp, skull and intracranial surfaces down-sampled to 2562 equidistant vertices each. Co-registration of the position of the EEG electrodes with the model was performed by projecting (with Brainstorm tools (5)) the co-registered locations of the same set of

electrodes with a slightly bigger (7-weeks-old) infant anatomy (6) on our newborn head model. Since an accurate segmentation of the cortical gyri was not possible (due to contrast and resolution issues), a standard gyrated cortical surface ('Colin 27') was used as the source space in the model (7). Such cortical surface was rescaled into the infant brain size, smoothed (20%) to match with the cortical folding of a newborn, positioned to the original cortical surface in the individual's MRI and down-sampled to 8014 vertices. The forward model was computed by using the Symmetric Boundary Element Method implemented in the OpenMEEG software (8). Based on recent simulation and empirical studies on newborn head models, we set the following conductivity values: scalp 0.43 S/m, intracranial volume 1.79 S/m, and skull 0.2 S/m (7, 9, 10).

In order to obtain an estimate of the noise in the EEG signals that did not include any stimulus-related brain activity, we identified for each subject artifact-free data segments beginning 750 ms after the offset of each trial and ending at the onset of the distracter starting the following trial. Noise covariance was computed from these segments after application of the same pre-processing procedure used for the stimulus-related data.

Simulation of localized oscillatory cortical sources. To test the effective spatial segregation of the reconstructed source distribution subtending the facelike pattern effect, we first selected a set of key, spatially separated cortical seeds by identifying the local maxima of t-values ($p < 0.005$) in the associated statistical map (Figure 3*C*). Five cortical seeds emerged in the right hemisphere (superior precuneus, posterior superior temporal sulcus, lateral occipital gyrus, anterior ventral temporal lobe, superior frontal gyrus) and one in the left hemisphere (retrocalcarine sulcus) (Fig. S2*A*). By using Brainstorm tools (5), we then simulated neurophysiologically plausible EEG recordings with an oscillatory source localized in each one of the seeds by performing the following steps:

1. We selected as surrogate background EEG recordings a 21 s-long segment of EEG data (the longest clean resting-state dataset, Subject 7) recorded during eyes-open rest in the absence of visual stimulation. These recordings have the same background 1/f-like power spectrum of original recordings and a duration corresponding to a short data epoch relative to the original recordings.

2. We generated localized oscillatory cortical sources consisting of purely sinusoidal signals at the stimulation frequency (0.8 Hz) in 1 cm^2 cortical patches (a neurophysiologically realistic surface extent) centered on each cortical seed and with the same duration of the surrogate EEG background recordings. These cortical signals were projected to the sensor space with the same forward model used for source reconstruction.

3. To obtain simulated recordings with a signal-to-noise ratio as close as possible to the one of the stimulus-related newborn's recordings, we added to the purely sinusoidal simulated recordings the surrogate EEG background recordings, with a proportional factor such that the resulting simulated recordings had a maximal (across channels) frequency-tagged response similar to the one of original stimulus-related EEG datasets (FTR≈10).

Spatial spread of the source reconstruction of simulated recordings. We reconstructed the sources of the simulated recordings and the source-level frequency-tagged response by applying the same procedure applied to the original data. Figure S2*B* shows the extent of the areas in which the amplitude of the frequency-tagged response is at least 1/3 of the local maximum. The spatial spread of each source is limited to a contiguous spatial neighbourhood.

Figure S1:

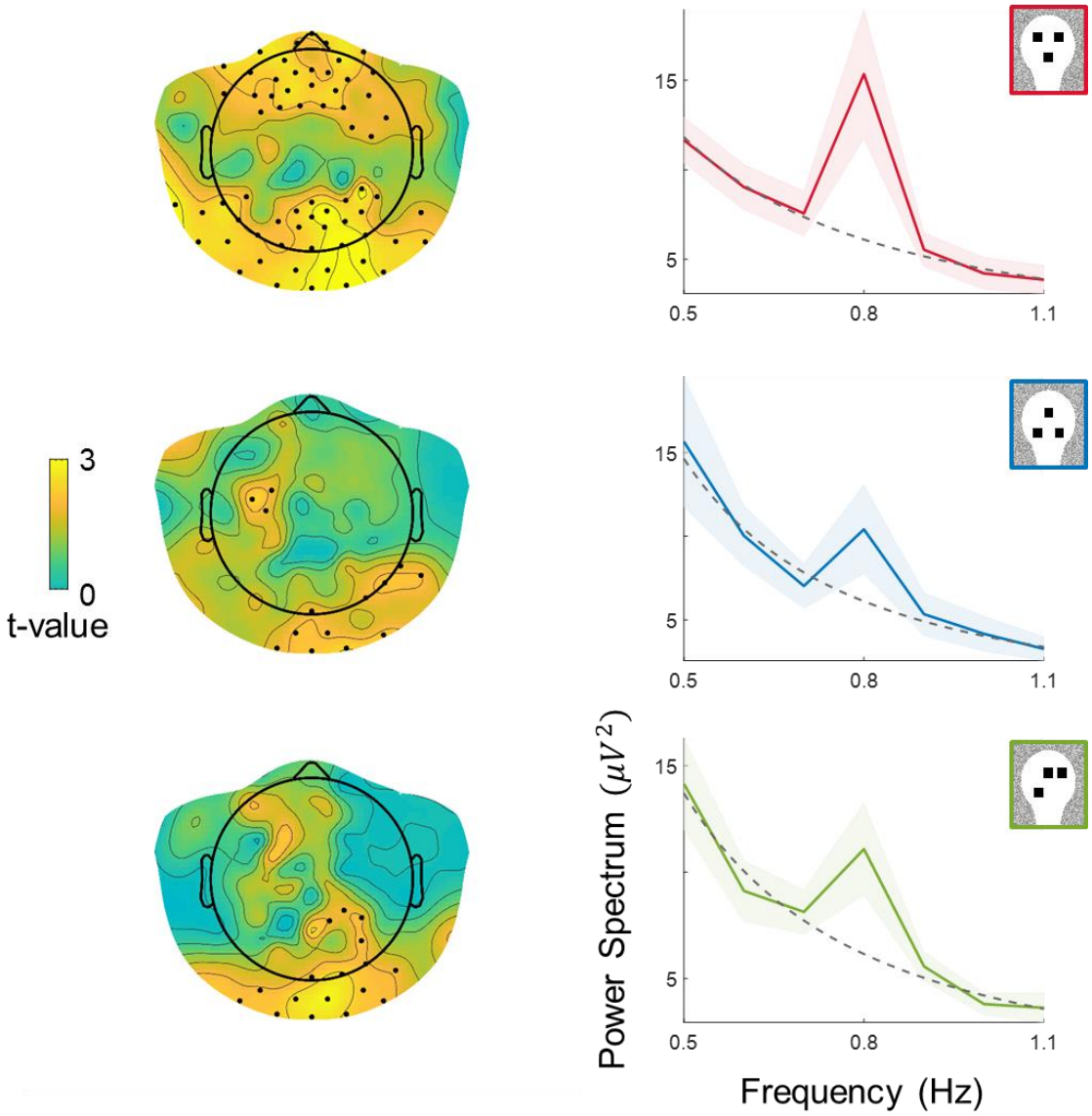

Frequency-tagged response for each condition.
First column: Statistical map (one-tailed *t*-test, corrected) of the difference between the power spectrum at the tag frequency (0.8 Hz) and the background power at the same frequency, estimated by a power-law fit of the power spectrum from the 6 neighboring frequency bins (±0.3 Hz). Electrodes belonging to a statistically significant cluster are marked with a black dot. All stimuli elicited a significant peak at the tag frequency in a posterior cluster (upright: P_{corr}<0.004; inverted: P_{corr} < 0.024; scrambled: P_{corr} < 0.020), while only upright stimuli gave rise to an additional peak in a frontal cluster (P_{corr} < 0.013). Second column: Power spectrum averaged over electrodes belonging to the posterior cluster (black line) ± s.e.m. across subjects (coloured shadow). The dashed dark-gray line indicates the power-law fit of the power spectrum (interval 0.5-1.1 Hz) for each condition.

Figure S2:

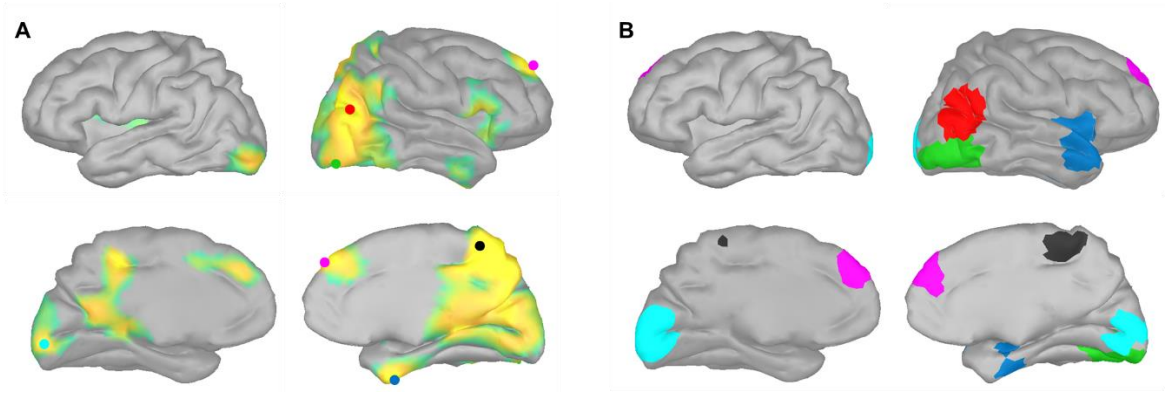

Spatial spreading of source-reconstructed simulated recordings from spatially localized oscillatory sources

(A) Location of cortical sources used for simulation (coloured dots), overlapped to the statistical map of the facelike pattern effect (lateral and medial view for each hemisphere); (B) Spatial spreading of the source-reconstructed frequency-tagged response for each simulated source (colours correspond to source locations marked in (A)): Each coloured area indicates the cortical extent within which the frequency-tagged response is > 33% of its maximum amplitude for that source.

Figure S3:

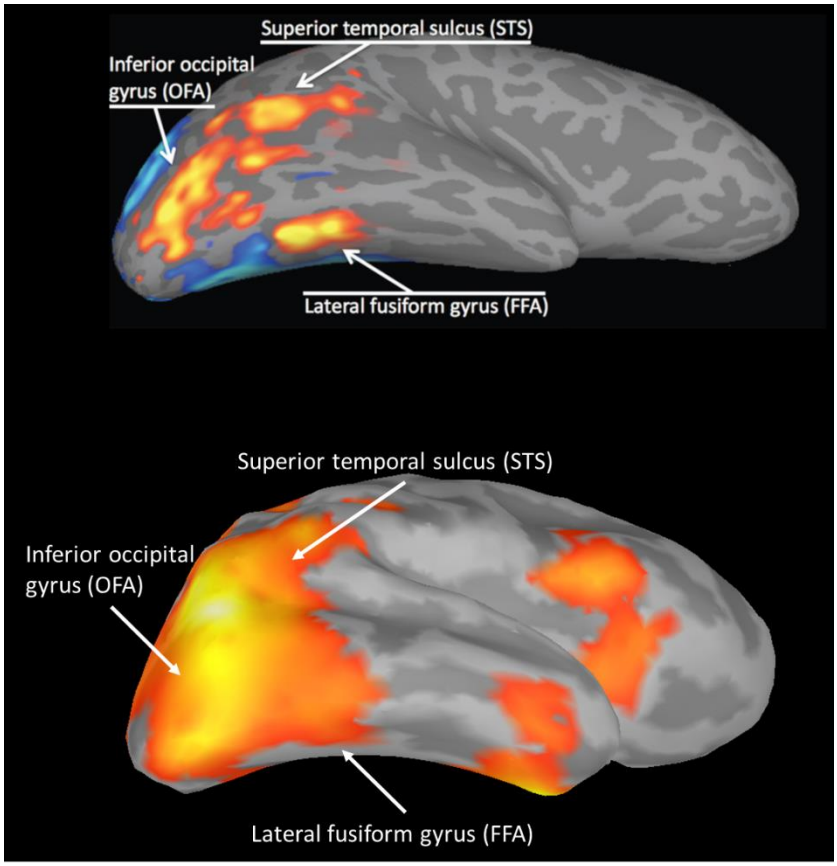

Comparison between newborn and adult face-selective cortical areas.
Upper panel: Cortical regions constituting the "core system" for visual analysis of faces in adults, reprinted from ref. (11), with permission from Elsevier and Oxford Publishing Limited through PLSclear; Lower panel: Cortical distribution of the facelike pattern effect (right hemisphere, lateral view tilted of about 45 degrees for comparison with upper panel). Acronyms: FFA=Fusiform Face Area, OFA=Occipital Face Area.

References

1. Brainard DH (1997) The Psychophysics Toolbox. *Spat Vis* 10(4):433–6.

2. Pelli DG (1997) The VideoToolbox software for visual psychophysics: transforming numbers into movies. *Spat Vis* 10(4):437–42.

3. Delorme A, Makeig S (2004) EEGLAB: an open source toolbox for analysis of single-trial EEG dynamics including independent component analysis. *J Neurosci Methods* 134(1):9–21.

4. Tokariev A, et al. (2018) Preterm Birth Changes Networks of Newborn Cortical Activity. *Cereb Cortex*:1–13.

5. Tadel F, Baillet S, Mosher JC, Pantazis D, Leahy RM (2011) Brainstorm: a user-friendly application for MEG/EEG analysis. *Comput Intell Neurosci* 2011:879716.

6. Kabdebon C, et al. (2014) Anatomical correlations of the international 10-20 sensor placement system in infants. *Neuroimage* 99:342–356.

7. Tokariev A, Vanhatalo S, Palva JM (2016) Analysis of infant cortical synchrony is constrained by the number of recording electrodes and the recording montage. *Clin Neurophysiol* 127(1):310–323.

8. Gramfort A, Papadopoulo T, Olivi E, Clerc M (2010) OpenMEEG: opensource software for quasistatic bioelectromagnetics. *Biomed Eng Online* 9(1):45.

9. Despotovic I, et al. (2013) Relationship of EEG sources of neonatal seizures to acute perinatal brain lesions seen on MRI: A pilot study. *Hum Brain Mapp* 34(10):2402–2417.

10. Odabaee M, et al. (2014) Neonatal EEG at scalp is focal and implies high skull conductivity in realistic neonatal head models. *Neuroimage* 96:73–80.

11. Haxby JV, Gobbini MI (2011) Distributed neural systems for face perception. *Oxford Handbook of Face Perception*, eds Rhodes G, Calder A, Johnson M, Haxby JV (Oxford Univ Press, Oxford), pp 93–109.